ARTICLE

Influence of Clearcoats on the Spectral and Physical Properties of Electrochemically Formed Colored Passive Layers on Zirconium

Andrew Munro,[†,‡] Michael F. Cunningham,[‡] and Gregory Jerkiewicz*

Department of Chemistry, Queen's University, 90 Bader Lane, Kingston, Ontario K7L 3N6, Canada, and Department of Chemical Engineering, Queen's University, 19 Division Street, Kingston, Ontario K7L 3N6, Canada

ABSTRACT We report on the application and characterization of two commercial polymer clearcoats to electrochemically formed colored passive layers on zirconium with the aim of providing effective physical and chemical protection while allowing the unique and colorful appearance of the colored passive layers to show through. Thin layers of an acrylic automotive clearcoat (~3.5 μm thick) and an epoxy marine clearcoat (~8.5 μm thick) were applied to the colored zirconium surfaces via spin coating and were found to only slightly modify their visual properties, maintaining their vibrant colors. As clearcoats were applied, the outer surface was found to be smoother than the surface of colored zirconium, thereby reducing potential wear from friction and the adhesion of fine dirt. Clearcoat-protected samples were found to wet less easily than colored zirconium alone, thus furthering its protection against damage in ambient (surface weathering) and aqueous media (aqueous corrosion). Light microscopy experiments at a 50−400× magnification revealed the absence of any structural defects in the clearcoats. The clearcoats show the ability to protect colored zirconium from physical and chemical damage, with the automotive clearcoat exhibiting superior adhesion. Our electrochemical coloring combined with the application of clearcoats creates a novel system that possesses unique esthetic properties while simultaneously offering protection against various forms of environmental damage such as weathering or corrosion.

KEYWORDS: zirconium • electrochemical coloring • electrochemistry • clearcoat • visual properties • surface morphology • adhesion

INTRODUCTION

Zirconium (Zr) is a metal traditionally used in the nuclear and chemical industries, yet increasingly finds new applications as a structural material in recreational items (bicycle frames, lacrosse sticks, etc.) and larger scale construction (chemical plant structures) because of its inherent strength, superior corrosion resistance, and low coefficient of thermal expansion. Previous work from this laboratory (1–3) has shown that the electrochemical passivation of Ti and Zr via an alternating current (AC) polarization increases the thickness of their passive layers, offering superior protection against corrosion and physical damage while causing the metals to exhibit a wide range of bright, uniform, and reproducible colors that are related to the passive layers' thickness. The unique colors are suitable for new and current applications that require the above-mentioned physical and chemical properties coupled with attractive visual characteristics. Because Zr solidifies with a smaller grain structure than Ti, it offers a smoother and shinier finish when chemically etched. Electrochemical anodization of Zr is a well-established technique (4–7) that employs direct current (DC) anodic polarization to passivate the metal. It is used in the fabrication and structural modification of zirconia (zirconium dioxide, ZrO_2) films, yielding a broad spectrum of useful materials ranging from nanoporous catalysts (8–10) to materials for photonic applications (11, 12). Our passivation method, which employs AC polarization in aqueous Na_2SO_4 solution at 10% w/v as the electrolyte, produces a broader spectrum of uniform and bright colors than does the DC polarization, and the AC voltage required to form them is lower than the respective DC one (3, 13).

Whether in decorative or structural applications, colored Zr would benefit from the protection offered by a stable and transparent polymer coating. The successful application of such a coating that physically protects Zr, while allowing the unique colors of the passive layers to show through, would introduce a novel method of protecting the colored layers without altering the visual properties of Zr. This is important because paints commonly used to color and protect metallic structures reveal poor adhesion to the Ti-group metals (such as Zr or Ti) (14, 15). In this paper, we report on the application and characterization of two commercial polymer clearcoats to electrochemically colored Zr. The first is an acrylic automotive clearcoat that is transparent and possesses chemical properties tailored to withstand weathering. The second is an epoxy marine clearcoat that is also transparent and exhibits mechanical and chemical stability in marine (seawater) environments (16). Spin coating was the application technique used, as it is suitable for small substrates and typically produces smooth, uniform coatings.

Acrylics boast an excellent durability and inertness, as well as impressive transparency. They also offer high gloss,

* Corresponding author. E-mail: gregory.jerkiewicz@chem.queensu.ca.
Received for review November 25, 2009 and accepted February 17, 2010
† Department of Chemistry, Queen's University.
‡ Department of Chemical Engineering, Queen's University.
DOI: 10.1021/am9008314
© 2010 American Chemical Society

Published on Web 02/26/2010

toughness, aging stability, and durability in ambient conditions (17). Acrylics are mostly used as the final coat on automobiles, refrigerators, and other industrial and domestic products requiring a durable, long-lasting coating. Epoxies are popular as protective coatings because of their excellent adhesion and broad chemical resistance, even in seawater environments. They create very hard coatings and make for a good machinery finish (17). They offer strong resistance to acidic and alkaline solutions, and most solvents.

The objectives of this work were the successful application of the clearcoats and the characterization of the coating/substrate systems with particular attention being paid to the modification of the physical properties of the colored layers brought about by the clearcoat layer. The characterization consisted of (i) determining the thicknesses of the clearcoat layers by using surface profilometry; (ii) analyzing changes to the visual properties of the colored layers brought about by the clearcoats by using visible light (vis) spectrometry; (iii) monitoring changes in the surface topography of the colored layers by topographical mapping; (iv) analyzing changes of the wetting properties of the colored layers through static water contact angle measurements; and (v) determining the adhesion of the clearcoats to the colored layers.

EXPERIMENTAL SECTION

Zirconium Sample Preparation. Disc-shaped samples were employed as electrodes and substrates. The Zr discs were made of commercially pure Zr (Alfa Aesar, 99.2 wt % purity on metals basis excluding Hf that always accompanies Zr; the maximum amount of Hf does not exceed 4.5 wt %) and were 11.0 mm in diameter and 1.0 mm thick with a total geometric surface area (A_g) of 225 mm^2. They were degreased in acetone under reflux and chemically etched in an aqueous solution of 13% v/v HF (Aldrich, 48 wt. % purity) and 44% v/v HNO_3 (Caledon, 68−70 wt % purity) (18). The "as-received" discs were only degreased and were not chemically etched or colored. The automotive clearcoat was Nason SelectClear Fast Flash Clearcoat 496−00 (automobile clearcoat, DuPont Canada Inc.), which is an acrylic coating cross-linked by a polyisocyanate activator (ratio of 4 parts polymer to 1 part activator); its exact chemical composition is proprietary. The marine clearcoat was EpoxyKote Clear 72 000 (National Epoxy Coatings), which is an epoxy coating cross-linked by a polyamide activator (ratio of 1 part polymer to 1 part activator); again, its exact chemical composition is proprietary.

Electrochemical Coloring. The electrochemical coloring of all Zr discs was conducted in a temperature-controlled single-compartment Pyrex electrochemical cell with an electrolyte of 10% w/v aqueous Na_2SO_4 (Aldrich, 99+ wt % purity) maintained at 298 ± 1 K and a large Pt (Alfa Aesar, 99.9 wt % purity) counter electrode. The coloring employed AC polarization (California Instruments 3 kVA AC Power Source, Model 3001 iM AC power supply) at a fixed AC voltage with a frequency of 60 Hz for 10 s (18). A distance of ca. 5 cm was maintained between the working and counter electrodes, and the electrolyte was vigorously stirred with a magnetic stirrer. This procedure ensured excellent reproducibility of the experimental results. All voltages referred to in this work are AC.

Application of Clearcoats. The acrylic and epoxy polymer clearcoats were applied to the Zr discs utilizing a spin-coater. The clearcoat solutions were applied to the flat face of the discs with a filtered (PTFE membrane filter, Whatman Inc., 0.45 μm pore size) syringe (1.0 cm^3 luer-slip syringe, National Scientific Co.) so as to cover the entire face. The disk was then rotated about its center at a speed of 4000 rpm for 20 s leaving a thin, uniform clearcoat layer that was allowed to cure in a dust-free environment. This speed and spinning time created the smoothest films while maintaining a suitable thickness (lower velocities gave a thicker coating that was rippled and higher velocities produced coatings that were too thin).

Light Microscopy Analysis. The surface morphology of the uncoated and coated colored layers was investigated using a light microscope (Seiwa Optical SDMTR, incandescent white light source: 20 W and 6 V) at different magnifications in the 50−400× range.

Visible Light Reflectance Spectrometry Measurements. The setup used for the acquisition of visible (vis) reflectivity spectra included a high-resolution spectrometer (Ocean Optics Inc. HR 2000 CG−UV−NIR) capable of detecting in the 200−1100 nm range with a wavelength (λ) resolution of 2 nm and an intensity (I) resolution of 3.2 counts (1 count ≈ 50 photons). It included a 300 μm high-SR fiber optic cable used to transmit the reflected light to the spectrometer. A 100 W incandescent white light source (emitting in a λ range of 408 to 1023 nm) was used as the visible light source and was shone at the disk surface at an angle of 45°. The detecting fiber was aimed at the disk surface at an angle of −45° (a 90° angle with respect to the light source) in order to detect the specularly reflected light. There was no detectable change in the wavelengths of the reflected light with a change in the angle of incidence. The software utilized to collect the data was 00Ibase32TM version 2.0.1.4 (Ocean Optics Inc.). During the data collection, an integration time of 200 ms was employed, along with an average of 50 acquisitions and a boxcar average of 10 data points. The uncertainties associated with reflectance measurements include any loss of information along the fiber-optic cable, as well as the undesired detection of any scattered or diffusely reflected light. It should be noted that the polished tip of fiber optic cables such as the one employed in this research typically transmits ca. 96% of incoming light (ca. 4% of incoming light is back-reflected).

Surface Profilometry Measurements. The surface profiler used for the clearcoat thickness analysis and surface roughness measurements was a Dektak 8 Stylus Profiler (Veeco Instruments Inc., vertical resolution of 40 nm, horizontal resolution of 3.43 data points/μm) utilizing a stylus with a tip diameter of 12.5 μm. It should be noted that error may be associated with the representation of surface characteristics (mainly valleys in between peaks) smaller than the tip diameter. The arithmetic surface roughness (R_a) was calculated according to eq 1:

$$R_a = \frac{1}{L}\int_{x=0}^{x=L} |y|\,dx \qquad (1)$$

where L is the scan length and y is the vertical deviation of the surface from the mean height. The clearcoat thickness measurements required the removal of the clearcoat from half of the Zr disk prior to scanning the stylus. This was accomplished with acetone (~15 wipes with an acetone-soaked soft lab-wipe) in the case of the acrylic automotive clearcoat and a soft blade (gentle shaving until substrate was reached but not damaged) in the case of the epoxy marine clearcoat. These rather crude approaches were applied in order to minimize any physical damage to the colored layer while effectively removing the clearcoat. Although organic solvents can soften epoxies, no suitable solvent facilitates local removal of an epoxy clearcoat (within a millimeter scale range). As such, the application of a soft blade was the only option that allowed us to cut and remove a section of the protective polymer coating without damaging the colored layer. The clearcoat thickness was taken as the difference between the average height of the coated surface and the average height of the bare substrate, being careful to exclude

Table 1. Rating Criteria for the Adhesion of the Polymer Clearcoats to the Zr Substrates in the Cross-Cut Test

rating	description of failure[a]
5	no peeling or removal
4	trace peeling or removal along incisions or at their intersection
3	jagged removal along incisions up to 1/16 in. (1.6 mm) on either side
2	jagged removal along most of incisions up to 1/8 in. (3.2 mm) on either side
1	removal from most of the area of the "X" under the tape
0	removal beyond the area of the "X"

[a] The description of failure refers to the state of the coating after removal of the tape. A rating of 5 is ideal, with 0 being the worst.

Table 2. Rating Criteria for the Adhesion of the Polymer Clearcoats to the Zr Substrates in the Cross-Hatch Test

rating	description of failure[a]
5	the edges of the cuts are completely smooth; none of the squares of the lattice are detached
4	small flakes of the coating are detached at intersections
3	small flakes of the coating are detached along edges and at intersections of cuts
2	the coating has flaked along the edges and on parts of the squares
1	the coating has flaked along the edges of cuts in large ribbons and whole squares have detached
0	flaking and detachment worse than rating "1"

[a] The description of failure refers to the state of the coating after removal of the tape. A rating of 5 is ideal, with 0 being the worst.

irregularities at the substrate/coating boundary created during clearcoat removal.

Contact Angle Measurements. The static contact angle measurements were conducted using a VCA Optima apparatus (AST Products Inc., resolution of 0.1°) utilizing 1.5 μL sessile droplets of distilled water at 295 ± 1 K. It should be noted that experimental characteristics, such as environmental humidity, can affect the contact angle measurements. Therefore, experiments were conducted in a humidity-controlled environment.

Adhesion Testing. ASTM adhesion test D3359−02 is a standard means of evaluating coating adhesion in the Canadian automotive industry and consists of two tests: (i) the cross-cut tape test and (ii) the cross-hatch tape test. A different disk was required for each experiment as the technique is destructive. The tests were performed at a certified external laboratory (ACT Laboratories Inc., 273 Industrial Dr., Hillsdale, MI 49242−1078, USA) that routinely carries out such measurements for the main Canadian automakers. The cross-cut tape test consists of introducing two incisions into the clearcoat layer to form a cross that intrudes down to the metallic substrate. Permacel Brand 99 (ACT #286) tape is then applied over the entire coated face of the disk for 90 s and is subsequently removed. The failure of the coating upon removal of the tape is reported as described in Table 1. The cross-hatch tape test is identical to the cross-cut tape test with the exception that instead of two incisions being made in the form of a cross, numerous incisions in the form of a grid (10 × 10 incisions on each disk) are introduced. The failure of the coating for this test is reported as described in Table 2. The maximum uncertainty in these tests is ±1 rating unit.

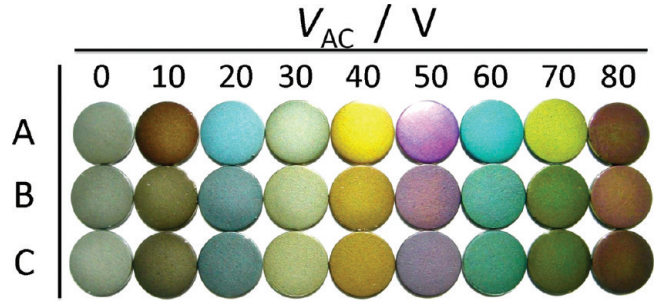

FIGURE 1. Coloration of passive layers on Zr prepared by the application of AC voltage (V_{AC}) in 10% w/v aqueous solution of Na_2SO_4; the passivation time is 10 s, the AC frequency is 60 Hz and the temperature is 298 K. The first column (V_{AC} = 0 V) shows noncolored samples without and with automotive and marine clearcoats. Row A, samples that are colored; row B, samples that are colored and protected with the automotive clearcoat; and row C, samples that are colored and protected with the marine clearcoat. The pictures were taken in outdoor lighting and the backgrounds (the spaces between and around the discs) were digitally removed in order to provide better contrast between the colors.

RESULTS AND DISCUSSION

Electrochemical Coloring of Zr and Clearcoat Application. The electrochemical coloring produces a colored passive layer on Zr (the native oxide covering the surface is removed by a chemical etching process that precedes the electrochemical coloring). It was found in previous studies that the thickness of the passive layers on Zr or Ti depends primarily on: (i) the applied AC voltage (V_{AC}); (ii) the frequency of the alternating current; (iii) the polarization time; (iv) the electrolyte concentration; and (v) the electrolyte temperature (2, 3, 13). In this article, we present results only for the variation of V_{AC}, the most influential variable, keeping the other parameters constant (see Experimental Section). Row A in Figure 1 shows the wide range of bright and uniform colors achieved by varying V_{AC} between 0 and 80 V; V_{AC} = 0 V refers to etched but uncolored Zr. Only results for $V_{AC} \leq 80$ V are presented as the application of higher voltages (with other parameters being the same) results in an electrical breakdown of the passive layer accompanied by visible and audible sparking that damages the protective layer (resulting in nonuniform coloration, crack formation and flaking). Once damaged by electrical breakdown, the film loses much of its visual properties and protection against corrosion. Each color (hue) is reproducible to the extent that it is difficult for one to visually distinguish between two discs treated at the same V_{AC}. The colors originate from thin film light interference (iridescence) (1, 2, 19–22). The rows B and C in Figure 1 present colored passive layers coated in automotive (Row B) and marine (Row C) clearcoat. It can be seen that the clearcoats only slightly affect the visual properties of the discs.

Light Microscopy Analysis. Optical micrographs of the colored passive layers on Zr before and after the application of clearcoats obtained at a magnification of 50× are shown in Figure 2. Although micrographs at higher magnifications (up to 400×) were recorded, we show only results for the 50× magnification as they well display and represent the overall trend. It can be seen that upon application of the

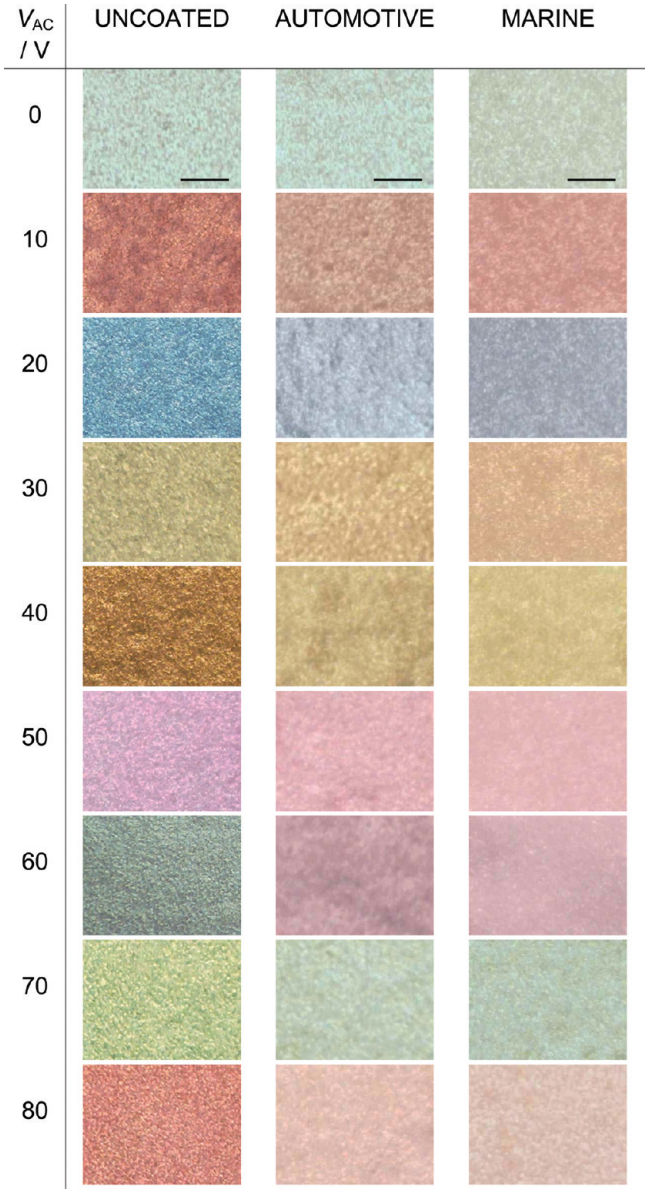

FIGURE 2. Optical micrographs of the colored passive layers on Zr formed at the indicated V_{AC} without and with clearcoats. The scale bars shown in the first row apply to all images and correspond to 500 μm.

clearcoats the color is slightly modified, often looking paler in comparison to the uncoated colored surface. The reason for this is described in the section dealing with the reflectivity analysis (see below). The morphology observed at this scale displays little if any change upon applying either of the clearcoats. Any morphological variations between surfaces of the same V_{AC} are attributed to original features resulting from the etching process. Though the micrographs of the coated surfaces reveal mainly the morphology of the underlying colored layer, as both the clearcoats are mostly transparent, it is likely that any imperfections (cracks, blisters, etc.) in the clearcoats would be detected by light microscopy. No such defects were found in the case of all the samples.

Characterization by Visible Light Reflectivity. The extent and mechanism in which the clearcoats affect the visual properties of the passive layers were investigated by recording reflectivity spectra in the visible (vis) region of

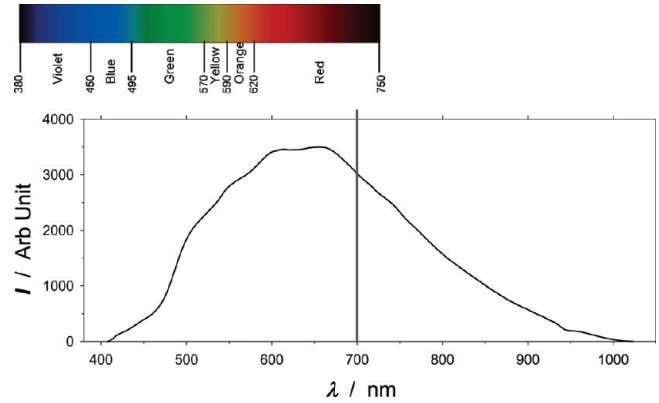

FIGURE 3. Emission spectrum of the white light source and a spectrum showing the assignment of colors to wavelength regions.

the electromagnetic spectrum. Figure 3 presents the emission spectrum (I vs λ) of the incandescent white light source (100 W) that also produces near-infrared (NIR) radiation. A gray vertical line is drawn to separate the vis region (400 nm $\leq \lambda \leq$ 700 nm) from the NIR one (700 nm $\leq \lambda \leq$ 1400 nm). The NIR region was excluded from the spectral analysis as it did not contribute to the visual characteristics that we study. It is interesting to observe a monotonous increase of I as λ increases from ca. 400 to ca. 650 nm. This behavior is characteristic of the light source that we employ because the detector gives the same response in different regions of the vis spectrum. The inset in Figure 3 shows the wavelength assignments for the primary colors of the vis region; it is used to relate the spectra of the colored passive layers to the coloration that they display. Figure 4 presents the reflectivity spectra of each colored layer on Zr, without and with either of the clearcoats. The reflectivity (R) is expressed as a fraction of the incident radiation reflected by a surface ($R = I_{refl}/I_{incid}$, where I_{refl} and I_{incid} are the reflected and incident spectral intensities). The spectra show R in the vis region, which is responsible for the color formation and visual properties. The data below 425 nm have been excluded from the reflectivity spectra as the signal in this region is weak, making the effects of uncertainty significant.

Figure 4A shows the reflectivity spectra for three samples: (i) etched Zr; (ii) etched Zr with an automotive clearcoat; and (iii) etched Zr with a marine clearcoat. Figure 4B–I shows the reflectivity spectra for four samples: (i) etched Zr; (ii) etched and colored Zr; (iii) etched and colored Zr with an automotive clearcoat; and (iv) etched and colored Zr with a marine clearcoat (the V_{AC} values for the respective layers are shown in the Figures). The spectrum for etched Zr (Figure 4A) refers to Zr covered with a very thin, oxide layer that develops upon contact of Zr with ambient conditions and is 2–5 nm in thickness; it is too thin to produce any light interference (23). The spectrum shows that etched Zr reflects over the entire visible region and the value of R gradually increases with increasing λ. The reflectance spectra for the colored but uncoated layers (Figures 4B–I) possess in some cases a wave-like shape (for $V_{AC} \geq 50$ V). The spectral peaks and valleys result from constructive and destructive interfer-

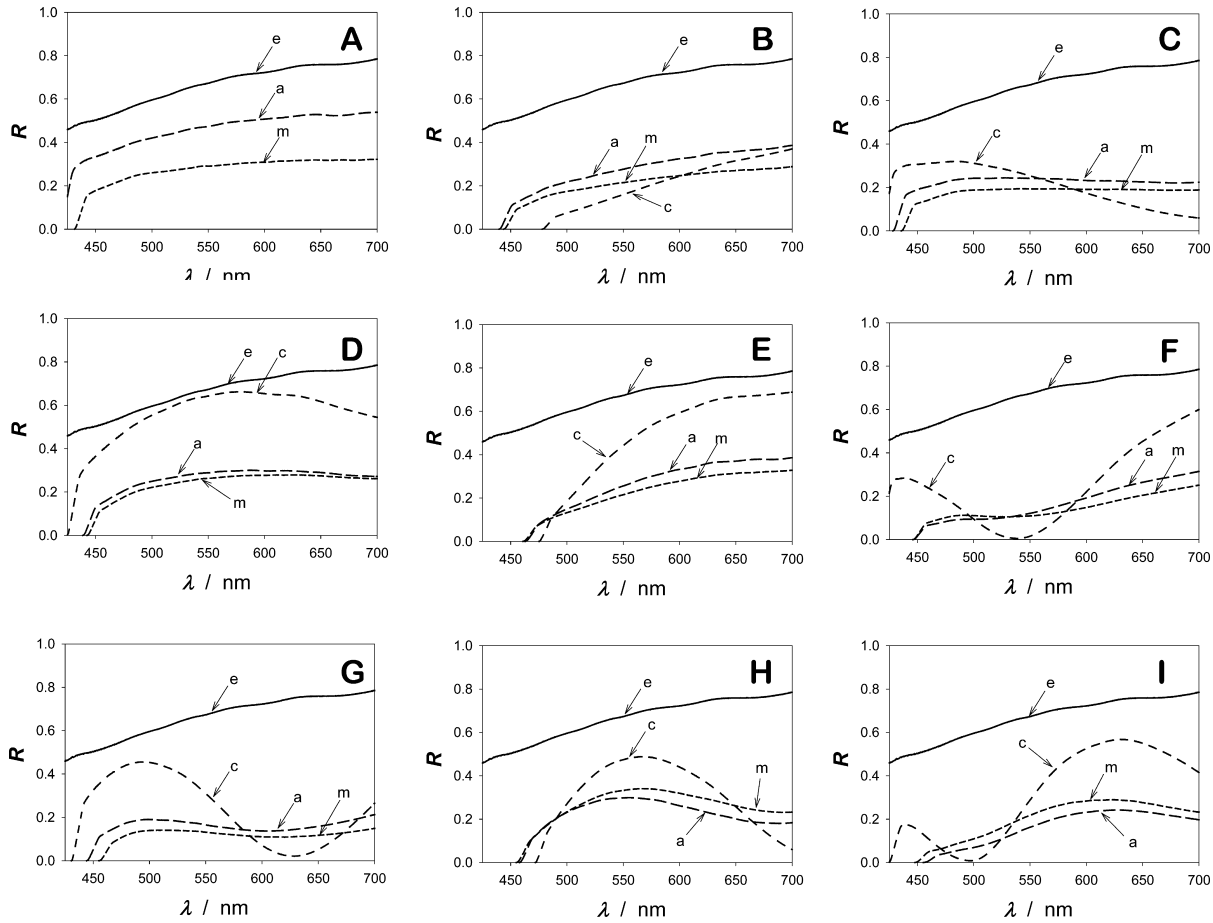

FIGURE 4. Sets of reflectivity spectra (R vs λ) for (A) etched Zr without and with clearcoats; (B–I) etched Zr, etched and colored Zr, and etched and colored Zr with clearcoats; the annotation e refers to the etched samples, c to the colored samples, a to the automotive clearcoat-protected samples, and m to the marine clearcoat-protected samples.

ence and vary in location depending on the thickness of the colored layer, which is related to the applied V_{AC}.

The spectral peaks correspond to color regions that are strongly reflected and therefore contribute largely to the overall observable color (in the case of two peaks, the resulting color is the product of the two contributions). Conversely, spectral valleys indicate color regions that are weakly reflected and are therefore absent in the observed color. However, not all spectra reveal well-defined peaks that can be assigned as the principal contributors to the resultant coloration. Instead, there are several colors that are reflected to an intermediate extent and contribute to the observed coloration. The wavelengths are assigned to colors using Figure 3, and the outcome of these assignments is summarized in Table 3, which lists the wavelength values of the maxima for each spectrum along with their corresponding colors, hence identifying the main components of each passive layer color.

The spectra of the colored, clearcoat-covered samples bear resemblance in shape to those of their uncoated counterparts, but their intensities differ for almost every wavelength in such a manner as to lower the spectral peaks and heighten the spectral valleys. This "flattening" of the reflectivity curves renders the spectra closer to that of white light (a perfect white light spectrum corresponds to a horizontal R vs λ line), causing the colors exhibited by the coated layers to be slightly paler with respect to the uncoated ones. This flattening effect is nicely displayed in the spectra shown in Figure 4G (colored layer formed at 60 V). In addition to the flattening, we also observe an overall reduction of R upon application of the clearcoats.

Table 3. Spectral Analysis of the Vis Region of the Reflectivity Spectra for the Zr Passive Layers

	peak(s) in vis region		
V_{AC} (V)	λ (nm)	R	main contributing colors
0 (etched Zr)	700	0.79	all
10	700	0.37	orange, red
20	484	0.32	violet, blue, green
30	576	0.66	green, yellow, orange
40	700	0.69	yellow, orange, red
50	437/700	0.28/0.60	violet, red
60	494/700	0.46/0.27	blue, green, red
70	567	0.49	green, yellow, orange
80	438/631	0.18/0.57	violet, orange, red

The application of clearcoats not only changes the shape of the spectra but also modifies the overall quantity of visible light reflected by the colored layers (interpreted as brightness), which is proportional to the areas under the reflectivity curves. An analysis of the spectra shown in Figure 4 clearly demonstrates that the area under a given reflectivity spectrum does not remain constant when a layer of either

Table 4. Effects of Clearcoat Application on the Total Quantity of Vis Light Reflected by the Zr Surfaces

	% change[a]	
V_{AC} (V)	automotive	marine
0 (etched Zr)	↓31	↓59
10	↑50	↑14
20	↑3	↓19
30	↓56	↓60
40	↓41	↓50
50	↓36	↓45
60	↓35	↓53
70	↓25	↓12
80	↓53	↓40

[a] The data are expressed as a percent change with respect to the total visible light reflected by the respective uncoated surface. Arrows refer to an increase or decrease in the total reflected light.

clearcoat is applied. The change of the intensity of the spectra is unique in each case (V_{AC} and clearcoat dependent). The area under each spectrum was integrated and taken to be the total visible light reflected by the corresponding colored layer. Changes to this value due to the application of either clearcoat are reported in Table 4.

The results presented in Figure 4 and Table 4 show that in most cases the coated surfaces reflect less visible light overall than their uncoated counterparts. A significantly opposite behavior is observed only for the colored layer formed at $V_{AC} = 10$ V. In this case, the reflectivity spectrum for the uncoated sample commences only at ca. $\lambda = 480$ nm, whereas in the case of the clearcoated samples, the spectra commence at lower λ values (440 and 445 nm). Because the clearcoats reflect a reasonable amount of light in the spectral region where the colored layer does not, this translates into greater brightness.

The data also reveal that the colored layers formed at $V_{AC} \leq 60$ V reflect more visible light overall when coated in automotive clearcoat than in the marine one. The opposite is true for the colored layers formed at $V_{AC} \geq 70$ V. It is interesting to observe that though the spectral intensity changes reported in Figure 4 and Table 4 are significant (as much as 60%), the changes observed by the naked eye are rather small (e.g., see Figure 1, $V_{AC} = 30$ V).

Determination of Clearcoat Layer Thicknesses. The thickness of the clearcoat layers was determined using stylus surface profilometry. The clearcoat layer was removed from half of each disk as described in the Experimental Section, creating a steplike feature at the half-disk boundary. The stylus was subsequently scanned from the bare substrate across the boundary to the coated surface, producing topographical data from which the thickness could be determined. To ensure reproducibility, the values reported below are averages of a minimum of 10 acquisitions on a minimum of 3 discs. Figure 5 shows a representative three-dimensional (3-D) image of the steplike feature for the colored layer formed at 60 V and covered with marine clearcoat. The image is created from the topographical mapping data collected by the profiler in a 3.0 mm × 4.0 mm scan area, though we show only the significant area around the feature (1.5 mm × 4.0 mm) as the rest is flat. The spikes or peaks are local imperfections caused by removal of the coating and are excluded from the data analysis. The clearcoat thickness is determined by equating it to the difference between the two average surface heights. It should be mentioned that vertical features are much smaller in reality than they appear in Figure 5 because the *z*-direction scale is of the order of several micrometers while the *x*- and *y*-direction scales are in the millimeter range (if the *z*-direction scale were to be the same as the others, the features would be ca. 1000× smaller).

The results of the thickness measurements are summarized in Table 5. Upon acquiring each thickness measurement, the arithmetic surface roughness R_a was calculated for the bare substrate and the coated surface using eq 1. The sum of these two R_a values is taken as the experimental uncertainty of each thickness. It is evident from the data that the substrate's initial state and coloration have little if any impact on the clearcoat layer thickness; the predominant parameter is the rotational speed during the clearcoat application. On average, the thickness of the automotive clearcoat is ca. $3.4 \pm 0.4\ \mu$m and that of the marine clearcoat is ca. $8.5 \pm 1.7\ \mu$m (the marine clearcoats are 2.5 times thicker than the automotive ones). Such values of thickness are typical of clearcoat applications on small objects, such as eyeglass frames, watches, cufflinks or other personal items, as they offer sufficient protection while avoiding added bulk. They would also be applicable for many decorative objects made of Zr (jewelry, ornaments, etc.). At this time, we have not investigated applying multiple layers of either clearcoat, nor have we investigated using other application processes. Should either of these processes prove capable of producing quality films, the ability to vary the clearcoat thickness would allow users to tailor the coating properties (hardness and UV filtration for example) to the object's end-use requirements.

Characterization of Surface Roughness. Surface roughness measurements were performed in order to determine changes in R_a brought about by the electrochemical coloring and the application of clearcoats. This was accomplished via surface profilometry measurements. The R_a values summarized in Table 6 are averages of at least 60 measurements across a minimum of 3 discs, and are for sample areas of 6.25 mm^2 (2.50 mm × 2.50 mm) and 0.16 mm^2 (400 μm × 400 μm). It is expected that "as-received", etched, and clearcoat-covered samples will reveal different surface morphological features intrinsic to the preparatory process. For instance, the "as-received" Zr samples should show scratches and rather small rolling hills and valleys, because they are prepared from an industrial-scale Zr sheet (3). On the other hand, chemical etching dissolves grains and grain boundaries at different rates, with the grain boundary dissolution rate being the fastest. Consequently, etched samples are expected to have a larger R_a value than the "as-received" ones, even though they might appear smoother to the naked eye and upon touch. Analysis of the large area

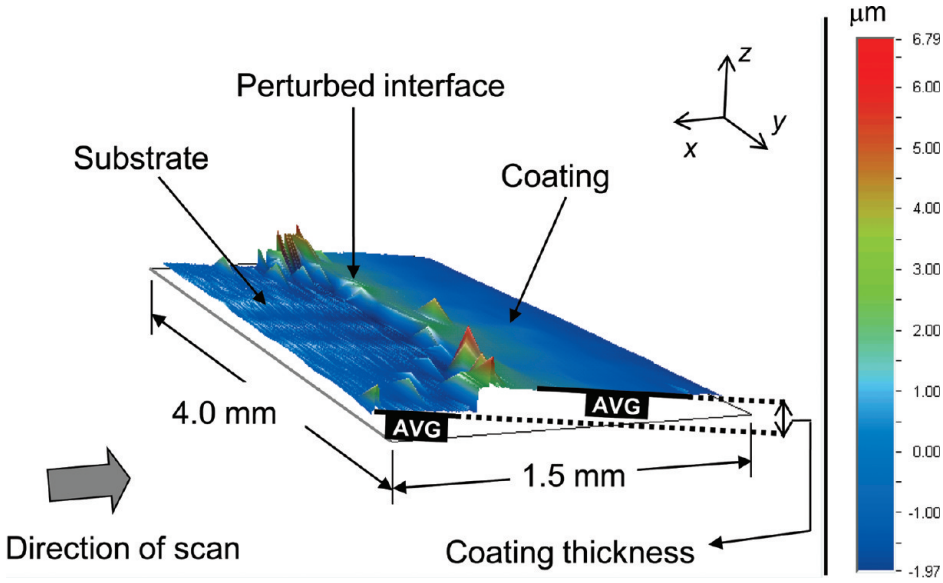

FIGURE 5. Three-dimensional image of the steplike feature at the marine clearcoat edge for the colored layer formed at V_{AC} = 60 V.

Table 5. Summary of the Polymer Layer Thickness Measurements on the Zr Surfaces

	automotive		marine	
V_{AC} (V)	thickness (μm)[a]	R_a (μm)[b]	thickness (μm)[a]	R_a (μm)[b]
as-received Zr	3.58 ± 0.33	0.28	8.35 ± 0.95	0.19
0 (etched Zr)	3.51 ± 0.43	0.37	8.62 ± 2.25	0.21
30	3.38 ± 0.38	0.29	8.52 ± 2.13	0.27
60	3.16 ± 0.38	0.28	8.34 ± 1.50	0.27

[a] Values reported are averages of a minimum of 10 acquisitions on a minimum of 3 discs and are presented with their standard deviations. [b] The R_a column indicates the uncertainty associated with surface roughness.

Table 6. Geometric Surface Roughness of the Zr Surfaces with and without the Clearcoats

		R_a (μm)[a]		
sample area (mm^2)	V_{AC} (V)	uncoated	automotive	marine
6.25	as-received Zr	0.22 ± 0.04	0.16 ± 0.02	0.22 ± 0.04
	0 (etched Zr)	0.63 ± 0.08	0.46 ± 0.10	0.34 ± 0.06
	30	0.43 ± 0.08	0.47 ± 0.09	0.42 ± 0.13
	50	0.44 ± 0.06	0.58 ± 0.12	0.48 ± 0.12
0.16	as-received Zr	0.16 ± 0.04	0.10 ± 0.06	0.04 ± 0.02
	0 (etched Zr)	0.20 ± 0.12	0.10 ± 0.03	0.06 ± 0.02
	30	0.16 ± 0.08	0.13 ± 0.06	0.09 ± 0.09
	50	0.18 ± 0.09	0.13 ± 0.07	0.07 ± 0.06

[a] R_a values reported are averages of at least 60 measurements across a minimum of 3 discs and are presented with their standard deviations.

(6.25 mm^2) reveals all surface characteristics (valleys, peaks, scratches, craters, large steps, terraces, etc.), whereas analysis of the small area (0.16 mm^2) shows only one of these features and the roughness variation within it. Therefore, R_a values obtained for large areas and for small ones are expected to vary. In Table 6, we present R_a values for a set of samples and although we report R_a for only two values of V_{AC} (30 and 50 V), they are representative of the overall trend.

From the "uncoated" column of Table 6, it can be seen that in the case of the 6.25 mm^2 sample area R_a increases upon chemical etching almost 3-fold (from 0.22 to 0.63 μm, a 186% increase) and then decreases upon coloring at 30 or 50 V by almost one-third (for V_{AC} = 30 V from 0.63 to 0.43 μm, a 32% decrease; for V_{AC} = 50 V from 0.63 to 0.44 μm, a 30% decrease). In the case of the 'as-received" sample, the chemical etching removes scratches and other defects that develop during the Zr sheet manufacturing (that includes rolling) and, subsequently, reveals the intrinsic grain structure. The subsequent decrease in R_a upon the electrochemical coloring is due to the formation of a colored passive layer that smoothes out the surface (1, 2). Preliminary data from our laboratory suggest that the colored layer is amorphous (13). The colored layer that develops on top of Zr masks its underlying crystalline structure and thus reduces R_a. Analysis of the 0.16 mm^2 area again reveals an increase of R_a upon chemical etching (from 0.16 to 0.20 μm, a 25% increase) and decreases upon electrochemical coloring at 30 or 50 V (for V_{AC} = 30 V from 0.20 to 0.16 μm, a 20% decrease; for V_{AC} = 50 V from 0.20 to 0.18 μm, a 10% decrease). However, these changes are smaller in magnitude because the roughness analysis in this range examines only a portion of one surface feature.

Upon application of the automotive clearcoat, R_a as examined for the sample area of 6.25 mm^2 decreases in the case of the "as-received" and etched samples (from 0.22 to 0.16 μm and from 0.63 to 0.46 μm, respectively) and increases in the case of the colored samples (for V_{AC} = 30 V from 0.43 to 0.47 μm; for V_{AC} = 50 V from 0.44 to 0.58 μm). In the case of the 0.16 mm^2 sample area, R_a decreases for all surfaces upon application of the automotive clearcoat; the change is the largest for the etched Zr sample (R_a decreases from 0.20 to 0.10 μm).

Upon application of the marine clearcoat, R_a as examined for the sample area of 6.25 mm^2 decreases significantly in the case of the etched Zr samples (from 0.63 to 0.34 μm)

Table 7. Static Contact Angle (θ) of 1.5 μL Sessile Droplets of Distilled Water (295 ± 1 K) with Zr Discs, Showing Effects of Passivation and Clearcoat Application

	contact angle θ (deg)[a]		
V_{AC} (V)	uncoated	automotive	marine
0 (etched Zr)	26.6 ± 3.0	91.9 ± 1.4	82.9 ± 1.4
30	62.5 ± 2.9	89.5 ± 2.3	81.3 ± 2.3
60	66.3 ± 2.6	89.7 ± 2.3	80.5 ± 3.4

[a] Values reported are averages of at least 10 measurements across a minimum of 3 discs and are presented with their associated standard deviations.

and remains almost the same in the case of the other samples. In the case of the sample area of 0.16 mm^2, R_a decreases in all cases by a factor of 2−4, depending on the sample and its pretreatment.

In general, the influence of the clearcoats on the surface roughness of the outer layer is found to depend on the inherent roughness of the substrate (initial state, chemical pretreatment, electrochemical treatment) and the characteristics of the clearcoat being applied (composition, thickness, density, viscosity, adhesion). In the case of the latter, there are two coating properties that dominate the clearcoats' surface roughness: (i) the inherent roughness of the cured coating finish itself, which is independent of the substrate but depends on the clearcoat composition; and (ii) the thickness of the applied clearcoat, as it determines the coating's ability to mask the substrate's topography (i.e., the thicker the layer, the less influence the substrate's roughness has on the R_a value of the outer layer). In the present case, the automotive and marine clearcoats differ in both of these coating properties, and hence affect the roughness of the outer layer to different extents. The marine clearcoat was found to not only cure to a smoother finish but also produce thicker layers (8.5 μm vs 3.4 μm), making it more capable of filling in any large defects (crevices, craters, valleys, scratches) in the underlying Zr surfaces. It is for these reasons that we see larger decreases in the surface roughness values of the outer layer upon applying the marine clearcoat than upon applying the automotive one.

Characterization of the Wetting Properties. The wetting properties of any metal or coated metal are instrumental in the control and prevention of its corrosion and surface weathering. It is preferable, with the exception of physiological applications (3), to have a surface that wets poorly in order to reduce its deterioration upon exposure to humidity and aqueous media. Poor wetting properties reduce the chance of water-induced degradation and damage. Table 7 summarizes the effects of the formation of the colored layers and the application of clearcoats on the static contact angle θ (deg) of water. The reported θ values are averages of at least 10 measurements across a minimum of 3 discs. The contact angle of pure Zr increases significantly from 26.6 to 62.5° (a 135% increase) and from 26.6 to 66.3° (a 149% increase) upon passivation at 30 and 60 V, respectively. The results show that the electrochemically formed colored layers have hydrophobic properties. As expected, one can also see that value of θ for all Zr surfaces increases when coated with either of the clearcoats, with the surfaces covered with the automotive clearcoat yielding higher θ values than those covered with the marine clearcoat by an average of ca. 9°. As all surfaces covered with the same clearcoat have roughly the same θ, it appears that the coloration does not directly influence θ to a significant extent once coated. As θ values increase upon electrochemical coloring and clearcoat application, it can be concluded that the wetting properties decrease. The procedure is beneficial in reducing water exposure to Zr, furthering its protection against corrosion and surface weathering.

Table 8. Summary of ASTM Standard Adhesion Test D3359-02 on Electrochemically Colored Zr Discs Coated in Automotive and Marine Clearcoat

		adhesion rating	
V_{AC} (V)	clearcoat	cross-cut	cross-hatch
as-received Zr	automotive	5	5
	marine	4	0
0 (etched Zr)	automotive	5	5
	marine	4	5
30	automotive	5	5
	marine	3	4
60	automotive	5	5
	marine	3	1

Characterization of the Adhesion of Clearcoats. Proper adhesion of the clearcoats to the Zr substrates is crucial in their ability to protect the underlying metal. Poor coating adhesion may allow for the formation of voids at the coating/substrate interface where liquids and gases can accumulate, consequently promoting damage (21). Moreover, a poorly adhered coating will likely chip, exposing segments of the substrate and facilitating numerous forms of physical and chemical damage. The adhesion of the clearcoats to the Zr substrates was examined with the ASTM D3359−02 adhesion tests (cross-cut and cross-hatch tape tests). The results of the testing are summarized in Table 8. The adhesion of the automotive clearcoat to all Zr surfaces was given the highest rating of 5 for both the cross-cut and cross-hatch tests, indicating that there was no failure of the coating. Though the strong adhesion is thought to be largely attributable to a suitable blend of surfactants in the clearcoat, resulting in good wetting and bonding of the clearcoat to the substrate, other factors such as the clearcoat's low viscosity and good mechanical adhesion also influence its bonding to the substrate. The adhesion rating achieved by the automotive clearcoat in these tests is what many leading automotive coating manufacturers demand from their coatings and, by their standards, deems the adhesion of the clearcoat to the Zr surfaces of adequate strength for use in automotive and possibly other applications. The marine clearcoat did not adhere as well, receiving adhesion ratings in some instances as low as 0, which denotes major coating flaking and removal during the test. As in the case of the automotive clearcoat, the adhesive performance of the marine clearcoat largely depends on its composition and surfactant content. We conclude that the marine clearcoat contains a surfactant

mix that is tailored in composition and quantity to steel and aluminum surfaces commonly used in marine environments, and is poorly matched to the relatively polar Zr surfaces (layers of ZrO_2 containing Zr^{4+} and O^{2-} always present on Zr) examined here. Evidence to support this hypothesis was the visibly poorer wetting of the marine clearcoat to the disk surfaces during its application compared to the ready wetting of the automotive clearcoat. This was noticeable by the higher contact angle of the marine clearcoat and its inability to spread over the entire disk surface, often receding from the edges after application. Another possible contributor to the marine clearcoat's comparatively inferior adhesion is its noticeably higher viscosity observed during application, making it more difficult for the coating to spread and mold to the topography of the surfaces, thus reducing contact and hence both chemical and mechanical adhesion. The marine clearcoat did however adhere relatively well to the etched Zr surface; this behavior can be associated with its higher R_a value.

Detailed discussion of the adhesion of either clearcoat to the colored layers on Zr with respect to molecular interactions at the clearcoat/colored layer interface is difficult, as the exact polymer composition of the clearcoat solutions is proprietary. The only constituent information made public is the identification of the solvents and the activators (see Experimental Section), along with the fact that the coatings are of the acrylic (automotive) or epoxy (marine) types. With the constituent polymer possibilities being numerous, prediction or discussion of the adhesion of the clearcoats in relation to the chemical composition and molecular interactions at the clearcoat/colored layer interface would be mostly speculative and is thus avoided.

CONCLUSIONS

The results have shown that a wide range of reproducible, unique, and well-defined colors can be prepared on Zr by electrochemical AC polarization in aqueous Na_2SO_4 solution. The subsequent application of a suitable polymer clearcoat can provide significant protection against damage without altering their visual properties in any major way.

Along with the visual benefits provided, electrochemical coloring and subsequent coating increase zirconium's protection from both chemical and physical damage. The former is achieved by significantly decreasing the wetting properties of Zr, thus reducing exposure to ambient and aqueous media. The latter is achieved by decreasing the roughness of the outer layer through creating a smoother surface and, consequently, reducing wear from friction and the adhesion of fine dirt. By providing the above benefits, our method offers the possibility of zirconium being a decorative metal that can be substituted for Ti in applications where a smoother, shinier finish is desired. No defects were detected in the clearcoat layers as examined by light microscopy and stylus surface profilometry, and the thicknesses achieved by spin-coating were in a range that makes them suitable for personal (eyeglass frames, watches, cufflinks) and decorative (jewelry, ornaments) applications. The acrylic automotive clearcoat exhibited excellent adhesion to the untreated and treated Zr surfaces, whereas the adhesion of the epoxy marine clearcoat is poor. Together, our electrochemical coloring and coating procedures create a promising and scalable technology that does not rely solely on the polymer coating for its appearance or its protection against corrosion or weathering.

Acknowledgment. We gratefully acknowledge financial support from the NSERC of Canada (Discovery Grant, Research Tools and Instruments Grants). A.M. thanks Drs. Hans-Peter Loock, Aris Docoslis, Robin Hutchinson, and Baodong Zhao for their helpful advice, as well as Mr. Gary Contant for his help in the preparation of the Zr discs.

REFERENCES AND NOTES

(1) Jerkiewicz, G.; Strzelecki, H.; Wieckowski, A. *Langmuir* **1996**, *12*, 1005.
(2) Hrapovic, S.; Luan, B. L.; D'Amours, M.; Vatankhah, G.; Jerkiewicz, G. *Langmuir* **2001**, *17*, 3051.
(3) Zhao, B.; Jerkiewicz, G. *Can. J. Chem.* **2006**, *84*, 1132.
(4) Leach, J. S. L.; Panagopoulos, C. N. *Electrochim. Acta* **1986**, *31*, 1577.
(5) Khalil, N.; Bowen, A.; Leach, J. S. L. *Electrochim. Acta* **1988**, *33*, 1721.
(6) Mogoda, A. S.; Heakal, F. E.; Ghoneim, A. A. *Thin Solid Films* **1992**, *219*, 146.
(7) Tsukada, T.; Venigalla, S.; Adair, J. H. *J. Am. Ceram. Soc.* **1997**, *80*, 3187.
(8) Tsuchiya, H.; Schmuki, P. *Electrochem. Commun.* **2004**, *6*, 1131.
(9) Tsuchiya, H.; Macak, J. M.; Ghicov, A.; Taveira, L.; Schmuki, P. *Corros. Sci.* **2005**, *47*, 3324.
(10) Tsuchiya, H.; Macak, J. M.; Taveira, L.; Schmuki, P. *Chem. Phys. Lett.* **2005**, *410*, 188.
(11) De La Rosa, E.; Diaz-Torres, L. A.; Salas, P.; Rodriguez, R. A. *Opt. Mater.* **2005**, *27*, 1320.
(12) Trivinho-Strixino, F.; Guimaraes, F. E. G.; Pereira, E. C. *Chem. Phys. Lett.* **2008**, *461*, 82.
(13) Bolduc, S. Coloured Passive Films on Zirconium, Titanium and Alloys: Preparation, Characterization, Applications. Master's Thesis, Queen's University, Kingston, ON, 2003.
(14) Dalard, F.; Montella, C.; Sohm, J. C. *Surf. Technol.* **1976**, *4*, 367.
(15) Dalard, F.; Montella, C.; Gandon, J. *Surf. Technol.* **1979**, *8*, 203.
(16) Munger, C. G. In *Corrosion Prevention by Protective Coatings*; NACE: Houston, 1984.
(17) Hamner, N. E. *Corrosion Basics: An Introduction*; NACE: Houston, 1984.
(18) Munro, A. J. The Application and Characterization of Protective Polymer Layers on Electrochemically Passivated Zirconium and Titanium. Master's Thesis, Queen's University, Kingston, ON, 2007.
(19) DelPlancke, J.-L.; Degrez, M.; Fontana, A.; Winand, R. *Surf. Technol.* **1982**, *16*, 153.
(20) Gaul, E. *J. Chem. Educ.* **1993**, *70*, 176.
(21) Schweitzer, P. A. *Corrosion Engineering Handbook*; Marcel Dekker: New York, 1996.
(22) Pérez del Pino, A.; Fernández-Pradas, J. M.; Serra, P.; Morenza, J. L. *Surf. Coat. Technol.* **2004**, *187*, 106.
(23) Jones, D. A. In *Principles and Prevention of Corrosion*; Johnstone, D. , Ed.; Macmillan: New York, 1992; Chapter 7, p 223.

AM9008314